Uranium Retention in a Bioreduced Region of an Alluvial Aquifer Induced by the Influx of Dissolved Oxygen

Donald Pan[†⊥], Kenneth H. Williams[‡], Mark J. Robbins[‡], and Karrie A. Weber*[†§]

[†] School of Biological Sciences, University of Nebraska−Lincoln, Lincoln, Nebraska 68588, United States

[‡] Lawrence Berkeley National Laboratory, Berkeley, California 94720, United States

[§] Department of Earth and Atmospheric Sciences, University of Nebraska−Lincoln, Lincoln, Nebraska 68588, United States

*Karrie A. Weber. E-mail: kweber@unl.edu; phone: (402)472-2739; fax: (402)472-2083.

Abstract

Reduced zones in the subsurface represent biogeochemically active hotspots enriched in buried organic matter and reduced metals. Within a shallow alluvial aquifer located near Rifle, CO, reduced zones control the fate and transport of uranium (U). Though an influx of dissolved oxygen (DO) would be expected to mobilize U, we report U immobilization. Groundwater U concentrations decreased following delivery of DO (21.6 mg O_2/well/h). After 23 days of DO delivery, injection of oxygenated groundwater was paused and resulted in the rebound of groundwater U concentrations to preinjection levels. When DO delivery resumed (day 51), groundwater U concentrations again decreased. The injection was halted on day 82 again and resulted in a rebound of groundwater U concentrations. DO delivery rate was increased to 54 mg O_2/well/h (day 95) whereby groundwater U concentrations increased. Planktonic cell abundance remained stable throughout the experiment, but virus-to-microbial cell ratio increased 1.8–3.4-fold with initial DO delivery, indicative of microbial activity in response to DO injection. Together, these results indicate that the redox-buffering capacity of reduced sediments can prevent U mobilization, but could be overcome as delivery rate or oxidant concentration increases, mobilizing U.

Introduction

Subsurface sediments are chemically and physically heterogeneous due to deposition and burial of soil horizons and surface derived organic material.(1,2) These organic-rich deposits represent an important facies type of subsurface sedimentary systems that generate reduced zones. The high concentrations of sediment-associated organic matter in the reduced zones generate “biogeochemical hotspots” distinct from the surrounding sediment matrix(3−5) and may result in diagentic retention of reduced chemical species including iron (Fe(II)) and contaminants such as uranium (U(IV)).(4−6) The reduction and oxidation of U plays a significant role in controlling U mobility.(5,6) Uranium mobility is primarily controlled by the very low solubility of solid-phase U(IV) minerals.(7) As such, biostimulation of U-

reducing bacteria has been used to immobilize U in subsurface systems.(8−11)

The stability of the immobilized U in these reduced regions depends on maintaining the immobile, reduced state rather than forming U(VI), which is highly soluble and complexes with carbonate.(12) The influx of oxidants, such as DO or nitrate, into reduced subsurface systems threatens long-term sequestration of U as U(IV)-bearing minerals by oxidizing and thus dissolving the minerals rendering U mobile in groundwater.(13) Though the influx of nitrate is often attributed to anthropogenic inputs,(14,15) DO infiltrates into reduced sediments through advective oxic groundwater flow as well as DO intrusion and transport from the capillary fringe.(16,17) Thus, the transitions between oxic and anoxic conditions can result in U geochemical changes as well as stimulation of microbial activity.(18−20) Organic carbon, H_2, or reduced minerals in these sediments can scavenge molecular oxygen and serve as a redox buffer.(21) The redox buffering capacity in reduced environments is not limited to abiotic reactions. Microbial activity has also been demonstrated to play a significant role in redox buffering in sedimentary environments by scavenging oxidants.(22) The effect of an influx of oxidants on reoxidation and remobilization of U *in situ* is not yet well understood. However, the prevailing hypothesis describes that an influx of oxidants (such as DO and nitrate) will oxidize reduced metals and radionuclides subsequently increasing U mobility.(23,24)

The influx of electron acceptors into reduced environments is recognized to stimulate microbial activity. Previous column studies indicate that upon exposure to an oxidant, reoxidation of bioreduced U(IV) occurs(21,25,26) along with changes to microbial population structures.(27,28)With increased microbial metabolic activity, virus production has also been observed to increase,(29) which could further contribute to carbon flux. Though the role of viruses in subsurface systems is poorly understood, viruses have been described to play a significant role in carbon cycling in marine and freshwater pelagic environments through the lysis of host cells during the process of lytic reproduction and the subsequent release of available carbon and nutrients.(30−32)Viruses have been detected via direct counts,(33−35) metagenomic data,(36,37) transcripts of viral proteins,(38) and electron microscopy(39) in shallow alluvial aquifers including U contaminated environments such as the U.S. Department of Energy (DOE) Rifle field site. Groundwater from organic rich regions of this aquifer also contained high viral loads, likely due to the greater microbial activity expected in organic-rich sediments.(35) Given the abundance of viruses in shallow alluvial aquifers, processes in the subsurface similar to those observed in surface waters can further drive biogeochemical cycling in subsurface systems and subsequently influence metal/radionuclide mobility. Though viruses have been demonstrated to be abundant in groundwater and subsurface environments,(29,40,41) the biogeochemical role they play *in situ* in subsurface sedimentary environments remains poorly characterized.

In an effort to investigate the effect of naturally occurring oxidant influx on the stability of U in a reduced aquifer we injected oxygen-saturated groundwater into a previously bioreduced experimental plot (U.S. Department of Energy (DOE) Rifle field site). The shallow unconfined alluvial aquifer contains U-bearing sediments that contribute to groundwater U concentrations that exceed the maximum contaminant level.
(42) Biostimulation of metal reducers by acetate injection has been used as a U remediation strategy in the Rifle aquifer and resulted in the successful removal of dissolved U from groundwater via the biogenic precipitation of reduced U(IV) minerals.(8−11) A byproduct of the *in situ* acetate injection was the accumulation of biomass and the production of artificially reduced sediments, creating a bioreduced zone in the aquifer.(43,44) In addition to U(IV)-bearing minerals, the bioreduced zone in this aquifer contains not only reduced soluble chemical species but also reduced minerals such as mackinawite (FeS) and framboidal pyrite (FeS_2).(5,8) These artificially bioreduced sediments share many similar characteristics with natural buried organic-rich sediment lenses, such as concentration of U(IV) and an abundance of iron sulfide minerals.(4,42) Thus, this bioreduced zone may be indicative of biogeochemical behavior in the wider Upper Colorado River Basin region where naturally reduced sediments are postulated to play a major role in the fate and transport of groundwater U.(42) The final acetate injection that generated the bioreduced zone was completed a year prior to the experiment described here. Here we collected groundwater from an upstream well, sparged the groundwater with air and injected back into a bioreduced region of the aquifer. The DO injection experiment lasted 123 days from August 18, 2012 to December 19, 2012. During this period, the injection was repeated, followed by an injection at a higher rate to increase the total amount of DO injected into the aquifer per unit time. Each injection was separated by pauses. Groundwater geochemical changes were monitored over time concurrent with cell and virus abundance as an assessment of microbial activity.

Materials and Methods

Field Site

The *in situ* field experiment was conducted on the DOE Rifle field site located 480 m east of Rifle, Colorado (USA). The site hosts a shallow, unconfined alluvial aquifer situated beneath a floodplain formed by a meander of the Colorado River. This aquifer is composed of Holocene-age alluvium consisting of sandy gravel and gravelly sand interspersed with silts and clays deposited by the river and overlying the Paleogene Wasatch Formation,(9,45) which serves as a local aquitard. The bottom 3–4.6 m of the alluvial sediments are saturated, but groundwater level fluctuates and can increase by as much as 1.5–1.8 m during periods of high runoff. Hydraulic conductivity is estimated to be 2–10 m/day with an average alluvium porosity estimated to be 15–35%.(46) The major source of groundwater in the aquifer is subsurface flow and recharge from the north, flowing southwest toward the Colorado River

(Figure 1) with localized spatial and temporal variations during high runoff. Additional minor contributions to groundwater flow potentially come from infiltration from an on-site ditch, recharge from precipitation, or hyporheic inflow of water from the Colorado River. Infiltration from the low permeability Wasatch Formation is deemed insignificant.(47) The groundwater is characterized as slightly reducing with DO concentrations typically less than 0.2 mg/L.(9,46) Further details of the Rifle site geology, hydrogeology and history are presented elsewhere.(8,46)

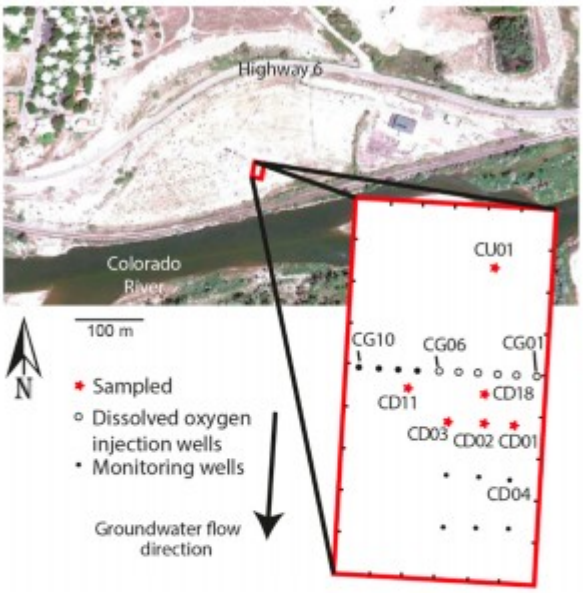

Figure 1. Map of experimental field Plot C within the U.S. Department of Energy's Rifle field site near Rifle, CO. Upgradient well CU01 was never bioreduced. CD wells were bioreduced in past field studies through acetate injections. In this study, groundwater containing DO was pumped into injection wells, CG01 through CG06, to introduce DO into the bioreduced region. Sampled monitoring wells CD18, CD01, CD02, and CD03, received the injectate. Samples collected from monitoring wells CD11 and CU01 represented regions of the aquifer that was not amended with DO injectate.

Aquifer Conditions Prior to Oxygenated Groundwater Injection

Biostimulation of the indigenous metal/radionuclide reducing microbial community with acetate created a bioreduced zone consisting of immobilized U within this aquifer. Generation of the bioreduced zone was accomplished through acetate injection over two successive field seasons (2010–2011; 2 and 1 year prior, respectively) into an experimental gallery (Plot C) as described elsewhere.(48,49) Plot C is oriented 190° azimuthal from north and generally oriented in the direction of groundwater flow at the time of the experiments (Figure 1). There, acetate stimulation of indigenous microorganisms led to the generation of a bioreduced zone characterized by elevated reduced Fe concentrations and immobilized U.(49,50)

Prior to the beginning of the experiment, neutral pH (7.2–7.5) groundwater was suboxic in all wells (DO concentration 0.05–0.11 mg/L; ORP −132– −196 mV) (Table 1) consistent with prior reports of aquifer conditions. (9,46,49,50) Wells within the bioreduced zone contained elevated aqueous (filtered through 0.45 μm PTFE membrane) ferrous iron (Fe(II)) and aqueous sulfide concentrations (3.4–5.1 mg/L and 9.59–63.26 μg/L, respectively), further supporting suboxic conditions within the aquifer (Table 1). This was in contrast to the upgradient well CU01 (unreduced region of aquifer), in which low Fe(II) and sulfide concentrations (0.27 mg/L and 1.92 μg/L, respectively) were observed (Table 1). Groundwater sulfate concentrations were similar among all wells (Table 1). Groundwater nitrate concentrations were not monitored over the course of the experiment but were measured below the detection limit in ca. 80% of background wells in Plot C with the highest concentration measured as 0.37 mg/L. Groundwater U concentrations varied between 66 and 201 μg/L, while Mn varied between 1.02 and 2.11 mg/L (Table 1).

Table 1. Groundwater Parameters Prior to Injection of Oxygenated Groundwater[a]

	CD18	CD01	CD02	CD03	CD11	CU01
DO	0.11 ± 0.11	0.07 ± 0.06	0.07 ± 0.06	0.07 ± 0.05	0.05 ± 0.02	0.09 ± 0.07
ORP (mV)	−132.72 ± 2.97	−131.95 ± 1.02	−143.68 ± 2.35	−183.14 ± 0.81	−191.59 ± 0.94	−162.33 ± 0.76
pH	7.68	7.67	7.46	7.45	7.35	7.65
Sulfide (μg/L)	23.02	63.26	55.6	49.861	–	9.59
Sulfate (mg/L)	957.7	984.6	935.6	915.5	928.0	941.4
U (mg/L)	0.119	0.156	0.066	0.195	0.176	0.201
Fe (mg/L)	11.5	6.760	7.360	4.330	3.980	1.490
Fe(II) (mg/L)	3.90	3.40	5.10	4.30	4.65	0.27
Mn (mg/L)	1.960	2.050	2.110	1.140	1.020	1.090
Viruses (/mL)	$2.50 \times 10^6 \pm 3.06 \times 10^5$	$2.60 \times 10^6 \pm 5.96 \times 10^4$	–	–	$2.12 \times 10^6 \pm 5.38 \times 10^5$	$2.58 \times 10^6 \pm 6.61 \times 10^4$
Cells (/mL)	$2.97 \times 10^5 \pm 2.59 \times 10^4$	$1.93 \times 10^5 \pm 4.17 \times 10^3$	–	–	$3.32 \times 10^5 \pm 7.36 \times 10^4$	$2.44 \times 10^5 \pm 6.25 \times 10^3$
Virus to Microbial cell Ratio (VMR)	9.43 ± 1.87	13.48 ± 0.60	–	–	6.38 ± 3.04	10.58 ± 0.54
DIC (Dissolved Inorganic Carbon) (mg/L)[b]	72.06	68.0	65.2	–	–	73.6
DOC (Dissolved Organic Carbon) (mg/L)[b]	0	6.0	7.0	–	–	3.6

[a]All measurements were conducted 16 days prior to injection except for DIC and DOC. U, Fe, and Mn were quantified in filtered (0.45 μm), acidified (HNO_3) samples by inductively coupled plasma mass spectrometry. Fe(II) was measured on filtered (0.45 μm) samples by the 1,10-Phenanthroline colorimetric method. Further details can be found in the Materials and Methods section. [b]Measurements conducted 37 days before injection.

Oxygenated Groundwater Injection

The oxygenated groundwater injectate was prepared by sparging groundwater with air until saturation with atmospheric O_2 and amended with a conservative tracer, deuterium (as D_2O; tank concentration δD = +240‰). The source of groundwater originated from an unamended well (CU01) and was pumped directly into a storage tank (18,000 L). Oxygenated groundwater was injected into the aquifer during three different periods separated by pauses between each injection period. Each injection and pause period is denoted by a numbered phase. In order to account for migration time, the phases in downgradient wells are delineated by tracer concentrations at each monitoring well. As such, the corresponding dates of

each phase vary between wells and are indicated on each figure. During Phase 1 of the experiment (days 0–23), oxygenated groundwater was injected into 6 injection wells (CG01–CG06) at a rate of 36 mL/min per well in order to achieve a final DO concentration of 2–2.5 mg/L. The injectate was circulated between adjacent wells using a peristaltic pump.(8) During Phase 2 (days 23–51), mineralization in the injectate line resulted in a decrease in the delivery of oxygenated groundwater as indicated by tracer concentrations (Figure S1). Later during Phase 3 (days 51–80), injection lines were checked periodically and cleaned to maintain flow rates. The injectate migrated through the aquifer, passing through downgradient wells. During Phase 4 (days 75–95), injection halted again, with a brief injection from day 79–85. On day 85, the brief injection was halted for tank refilling and equipment maintenance. During Phase 5 (days 95–125), the injection rate was increased by 2.5-fold (90 mL/min per well) in order to increase the aquifer DO concentration to ca. 5–6 mg/L. Because O_2delivery was achieved by groundwater injection, subsurface flow rates may have changed by less than 10 mL/h during the slow injection phase to less than 15 mL/h during the fast injection phase. However, water table levels did not rise in comparison to unamended controls (Figure S9A). Because of a temperature differential, the injectate slightly increased groundwater temperature no more than +1 °C before day 70 and no more than −2 °C after day 70 (Figure S8).

Several precipitation (rain and snow) events occurred over the course of the experiment with a maximum of 13 mm of precipitation recorded (Figure S9B). Days 5, 37, 55, and 84 were the only events associated with any considerable rise in the water table (Figure S9A).

Actual groundwater DO concentrations were measured along with ORP in purged wells using multiparameter sondes (detection limit 0.04 mg/L, YSI, OH). The amount of O_2 delivered was inferred from measured concentrations of the deuterium tracer quantified using a Liquid Water Isotope Analyzer (Los Gatos Research). The concentration of injected O_2 inferred for each well (that is the DO concentration if the injected O_2 were not consumed) was calculated by the ratio of D_2O measured in the well to the original D_2O concentration in the tank multiplied by the saturation concentration of DO at the water temperature:

$$\mathrm{DO}_{\mathrm{inferred}} = \frac{\mathrm{D_2O}_{\mathrm{measured}}}{\mathrm{D_2O}_{\mathrm{tank}}} \times \mathrm{DO}_{\mathrm{saturation},T}$$

The rate of O_2 delivery into each well was determined by the following equation:

$$\mathrm{O_2\ rate} = \frac{(\Delta\mathrm{DO}_{\mathrm{inferred}} - \Delta\mathrm{DO}_{\mathrm{out}}) \times V}{\Delta\mathrm{time}}$$

where V is the volume of the well, and ΔDO_{out} is the decrease in DO concentration due to flushing. ΔDO_{out} is calculated by the equation:

$$\Delta DO_{out}(t_i) = DO_{inferred}(t_i)e^{m(t_i - t_i)} - DO_{inferred}(t_i)$$

where *m* is the first-order rate of loss of the tracer determined by measuring the rate of loss of the tracer during Phases 2 and 4 when injectate delivery was stopped. Aqueous U concentrations in downgradient wells were corrected for the soluble U delivered by injection. Injected groundwater accounted for no more than 10% of sampled groundwater at its greatest extent during the slow injection phase and less than 18% during the fast injection phase.

Over the course of the experiment, groundwater samples for cation, anion, pH, and Fe(II) analyses were collected from certain wells. Effects of the O_2 delivery were studied in the four wells (CD18, CD01, CD02, CD03) closest in proximity to where the DO influx meets the bioreduced zone. These were compared to two controls: an upgradient control that had never received acetate amendments (CU01) and a control that was previously biostimulated with acetate but in which no O_2 is delivered (CD11) (Figure 1). Other parameters (DO, ORP, temperature) were measured *in situ* within the wells. Samples for cell and viral enumeration over the course of the experiment were also collected.

Geochemical Analyses

Samples for anion, dissolved inorganic carbon (DIC), and DOC analyses were filtered (0.45 μm PTFE) and stored at 4 °C in no-headspace HDPE (anion) and glass vials (DIC/DOC) until analysis.(51,52) Anions were measured using ion chromatography (ICS-2100, Dionex, CA) equipped with AS18 analytical columns.(53) Cations (U, Fe, Mn) were quantified using inductively coupled plasma mass spectrometry (Elan DRCII ICP-MS, PerkinElmer, Inc.) following filtration (0.45 μm PTFE) and acidification (0.2 mL 12 N HNO_3 per 20 mL sample). Total cation groundwater concentrations will include submicron colloids less than 0.45 μm. Ferrous iron concentrations were measured on filtered samples (0.45 μm PTFE) immediately in the field upon sampling using the 1,10-Phenanthroline colorimetric method (Hach Company).
(54) Sulfide was measured spectrophotometrically immediately upon sampling using the methylene blue method (Hach Company).
(55) Measurements for DIC/DOC were made on a Total Organic Carbon Analyzer (TOC-VCSH; Shimadzu, Corp.). DOC was obtained as the difference between total dissolved carbon and DIC. Spearman's correlation analysis was conducted to test the relationship between O_2 consumed within the aquifer and change in abundance of U and other aqueous cations. All statistical computation was conducted using GraphPad Prism (v5.02, GraphPad Software, Inc.). Significance level for the regressions was chosen at a *P*-value of <0.05.

Cell and Virus Collection for Enumeration

Prior to sample collection, wells were purged (12 L; ca. 1–1.5 well volumes) with a peristaltic pump (ca. 50 mL/min). Samples were immediately filtered through low protein-binding PVDF filters (0.45, 0.22, and 0.1 μm pore size; Millipore SLHV033RS, SLGV033RS, and SLVV033RS, respectively) to produce <0.45 μm, <0.22 μm, and <0.1 μm size fractions. DNase I (10 U/mL final concentration) was added to remove free and particulate DNA. Samples were subsequently fixed with electron microscopy grade glutaraldehyde (0.5% final concentration) for 15–30 min at 4 °C and frozen in liquid N_2.(56) Fixed samples were stored at −80 °C prior to overnight shipment on dry ice to the University of Nebraska–Lincoln for enumeration. Cells and viruses were enumerated by epifluorescence microscopy using SYBR Green I (Life Technologies) as a nucleic acid stain (Supporting Information). Viruses, contained within the <0.1 μm fraction, were collected onto Anodisc filters (0.02 μm pore size, Whatman/GE Healthcare 6809-6002). Cells, within the <0.45 μm fraction, were collected onto 0.2 μm black polycarbonate filters (Millipore GTBP02500). Epifluorescence enumeration was conducted on an epifluorescence microscope (Axioskop 40, Zeiss) with mercury lamp (Osram, HBO50W.L2) and 35001v3 filter cube (Chroma). At least 10 fields or 200 counts were enumerated per filter.(57) When monitored over time, the virus to cell ratio may reflect changes in underlying ecosystem properties including microbial activity.(58)

Planktonic cell and viral abundance prior to the experiment ranged from 1.9 to 3.3 × 10^5 cells/mL and 2.1–2.6 × 10^6 viruses/mL, respectively (Table 1). Planktonic cell and viral abundance in upgradient well CU01 measured 2.4 × 10^5 cells/mL and 2.6 × 10^6 viruses/mL, respectively, resulting in a virus-to-microbial cell ratio (VMR) of 10.6 (Table 1). VMR ranged from 6.4 to 13.5 in sampled wells within the bioreduced zone (CD18, CD01, and CD11) (Table 1).

Results

Phase 1: Initial O_2 delivery

Fluctuations in groundwater biogeochemistry were observed with the injection of oxygenated groundwater into the bioreduced zone of the aquifer during Phase 1. Despite the injection of oxygenated groundwater, DO concentrations measured in the downgradient wells remained low (<0.2 mg/mL; initial DO concentration 0.05–0.11 mg/L) (Figure 2A,B). If DO had not been consumed, up to 0.8 mg/L DO may have been expected based on tracer concentrations. The low DO concentrations were not solely the result of dilution but rather the consumption of DO before the injectate (as indicated by the tracer) arrived at the monitoring wells (Figure 2A,B). Consumption of DO is further supported by a decrease in measured ORP values starting on day 6–10 from −146– −132 mV to −317– −304 mV by day 19 (Figure 2E,F). On day 19, decreases in ORP values were also observed in control wells, however this only occurred after ORP had already started decreasing in downgradient wells. Groundwater sulfide concentrations, higher relative to controls, varied in their response to the oxygen injection

(Figure S3). Sulfate concentrations fluctuated similarly in all wells (Figure S3). Following the DO injection into treatment wells, aqueous U concentrations also decreased, while groundwater U concentrations remained constant in unamended control wells (Figure 2I–L). Interestingly, during this same period, significant fluctuations in groundwater DOC as well as DIC concentrations were observed in treated downgradient wells (Figures 2U–W and S5). Though DIC concentrations in the upgradient control well CU01 also fluctuated, DOC concentrations did not signficantly change (Figure 2W). Total Fe (fraction <0.45 µm) decreased during Phase 1 and was negatively correlated with the mass of DO consumed (Figures 3 and S2). Measured groundwater Fe(II) concentrations were not significantly correlated to DO. Similar to total Fe, total Mn concentrations were also negatively correlated with DO consumption (Figures 3 and S2).

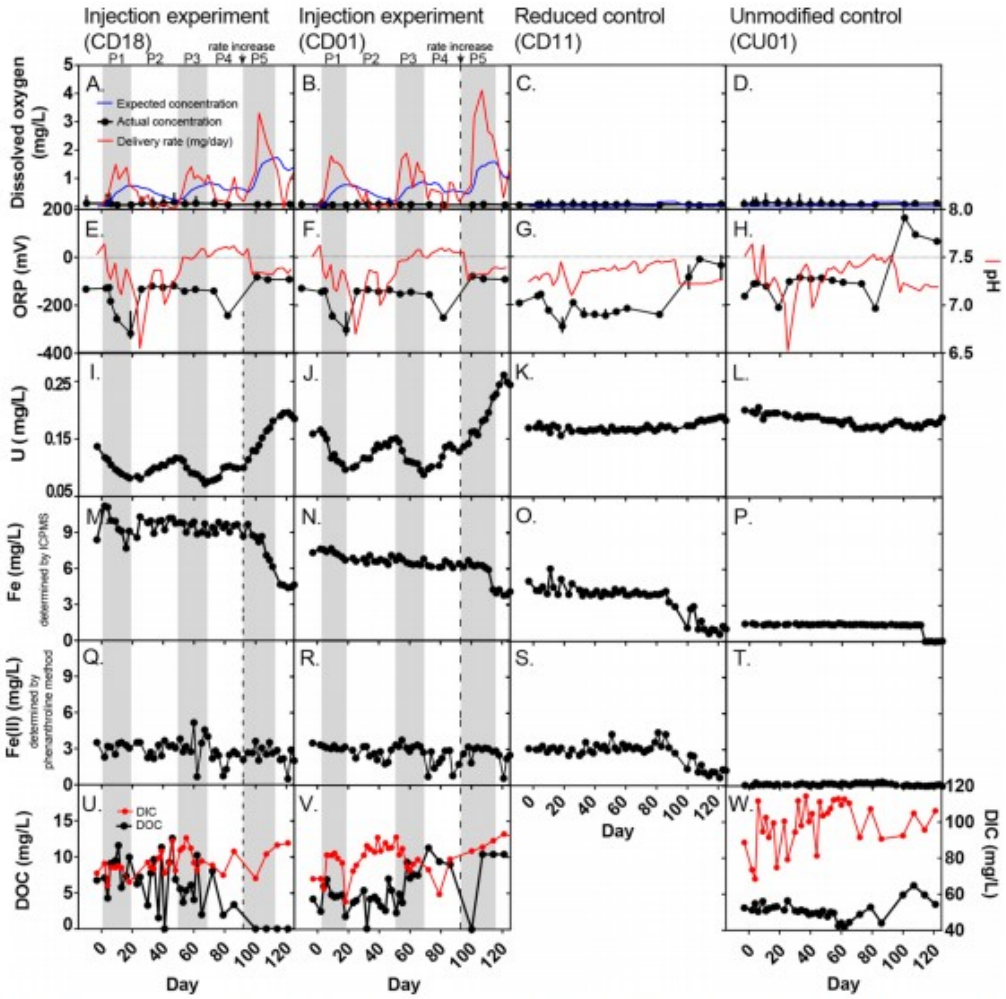

Figure 2. Chemical changes over time following DO delivery into the bioreduced zone of the aquifer: (A–D) DO, (E–H) ORP and pH, (I–L) U, (M–P) total Fe measured by ICPMS, (Q–T) Fe(II) measured by the phenanthroline colorimetric method, and (U–W) DOC/DIC. DO and ORP data bars represent the range of measured values from the top to the bottom of the well column. P1–P5 represent the phases of the experiment. Shaded regions (P1, P3, P5) represent periods of oxygen delivery as determined by measured tracer concentrations. The vertical dashed lines indicate the period when the injection rate was increased from 36 mL/h per injection well to 90 mL/h. Data for wells CD02 and CD03 are displayed in the Supporting Information (Figure S5).

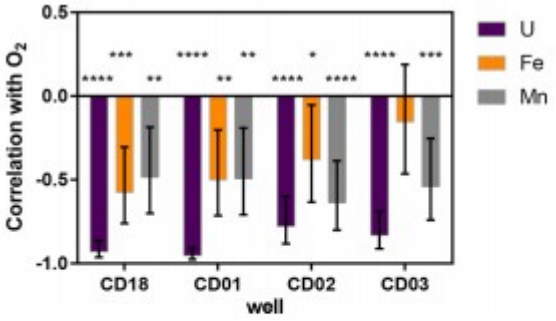

Figure 3. Spearman correlations between groundwater metals (U, Fe, Mn) and O_2 consumed in the well during the slow injection phase (P1-4). Stars represent the degree of significance with a single star (*) representing $p < 0.05$, two stars (**) representing $p < 0.01$, three stars (***) representing $p < 0.001$, and four stars (****) representing $p < 0.0001$. Details of the correlation are displayed in Figures 5 and S2.

The injection of DO resulted in an increase in virus abundance relative to the control wells that did not receive the DO injection, day 4 to 11 (Figure 4B). During this period, virus abundance and the virus-to-microbial cell ratio (VMR) increased relative to the control wells (Figure 4B). The virus abundance increased 136% and 71% in CD18 and CD01, respectively, while in the control wells, viral abundance increased only 7% (CU01) and 33% (CD11). In downgradient wells, the VMR increased 32% (CD18) and 44% (CD01), and in control wells the VMR only increased 3% (CU01) and 9% (CD11). The increases were not due to a higher load of viruses in the injectate. If the injectate were to account for the increase in viruses observed in CD18, nearest the injection wells, virus abundance in the injectate would have had to have been greater than those observed in the Colorado River. (35) Cell abundances would also be expected to increase. However, cell abundance remained relatively constant over the course of the experiment despite the influx of an electron acceptor and evidence of biogeochemical activity (Figure 4A). Viral abundance continued to increase in downgradient wells until it was 1.5 to 4-fold higher compared to the beginning of the experiment (1.1×10^6–2.1×10^6 viruses/mL to 2.3×10^6–4.6×10^6 viruses/mL) (Figure 4A). VMR in downgradient wells increased (1.8 to 3.4-fold) from 3.9 to 10.1 to a maximum of 11.0–17.9 (Figure 4A). An increase in virus abundance in control wells indicate that viral abundance can naturally fluctuate between sampling time points (approximately 1 week). While VMR in control wells fluctuate throughout the experiment, the highest increase was observed in downgradient wells immediately after DO injection. A 3-fold increase in virus abundance in CD11 (from $9.7 \times 10^5$to 2.9×10^6 viruses/mL) was also observed concomitant with a decrease in ORP (from −155 to −289 mV), similar to other wells from the bioreduced zone (Figures 2G and 4A).

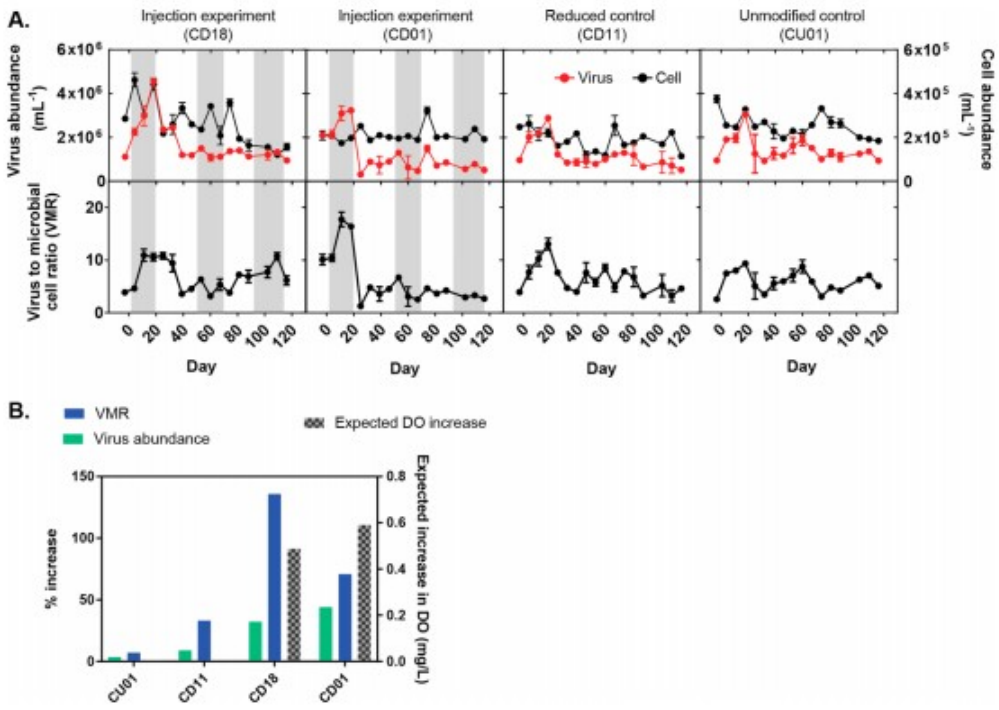

Figure 4. (A) Abundance of cells and viruses in groundwater. Viral/cell abundance and VMR error bars represent the standard error of duplicate measurements. (B) Effect of DO on virus abundance in downgradient wells CD18 and CD01 during the initial period of the injection from day 4 to 11. During this period, virus abundance and the virus-to-microbial cell ratio increased relative to the control wells.

Phase 2: Response after a Pause in O_2 Delivery

Delivery of oxygenated groundwater was paused on day 23 due to mineral precipitation in the injectate line. During the pause in oxygenated groundwater injection, groundwater DO concentrations remained below detection limits (<0.2 mg/L) (Figure 2A,B). However, the pause in oxidant delivery resulted in the shift from a reducing system (ORP −305 ± 11 mV) to a slightly more oxidizing (ORP −141 ± 6 mV) system and allowed the ORP to recover to preinjection levels (−148 ± 24 mV) (Figure 2E,F). The pH decreased during Phase 2 but did not correspond with ORP changes (Figures 2E–H and S5B). The pH reached as low as 6.5 in some wells, including CU01 (Figure 2E–H). The change in redox conditions is marked with a rebound in groundwater U concentrations back toward preinjection levels (Figure 2I,J), while groundwater Fe and sulfate concentrations also trended upward (Figures 2M,N, S2, and S3). A visual observation of orange-red mineral precipitates on membrane filters and appearance of orange-red mineral flocs in well casings from downgradient wells was observed when the ORP increased (Figure S4). The orange-red mineral precipitates are consistent with the precipitation of iron oxides that would occur in an oxidizing system.(59) Groundwater DOC concentrations continued to fluctuate within the wells of the bioreduced zone while DOC in the upgradient well CU01 remained low (1.9–4.0 mg/L) with little fluctuation (Figures 2U–W and S5F). DIC generally increased in downgradient wells as well as upgradient well CU01 during Phase 2 (Figures 2U–W and S5F).

During Phase 2, viral abundance decreased 50–90% (from a range of 2.–4.6 × 10^6 viruses/mL to 3.2–2.4 × 10^6 viruses/mL), concomitant with formation of orange-red precipitates consistent with minerals presumed to be Fe(III) oxides in groundwater (Figures 4A and S4). Because mineral surfaces can serve as attachment sites for the adsorption of viruses, the planktonic, unattached groundwater viruses that were measured in this study represent a subset of the total viral abundance present in the aquifer.(60,61) As such, after the onset of visible mineral precipitation during Phase 2, groundwater viral abundance is inferred to be suppressed due to adsorption onto newly precipitated mineral surfaces. After Phase 2, groundwater virus and cell abundance did not significantly change for the remainder of the experiment. VMR remained relatively low, ranging from 1.3 to 4.7 following the initial drop during Phase 2 (Figure 4A).

Phase 3: Response after Resumption of O_2 Delivery

The delivery of oxygenated groundwater resumed on day 51 and as observed with the initial injection (Phase 1), geochemical conditions shifted again. Aqueous U concentrations decreased and replicated the decrease in groundwater U concentrations observed after the initial delivery of DO (Figure 2I,J). Similarly, Fe and Mn concentrations decreased in accordance with the negative correlation with DO consumption in the sediment (Figures 3 and S2). As previously observed after the initial period of DO delivery, significant DOC fluctuations continued after day 51 (Figures 2U,V and S5F). However, in the upgradient well CU01, DOC only changed minimally, decreasing slightly to 0.4 mg/L and subsequently rising to 3.2 mg/L (Figure 2W). DIC concentrations also fluctuated (Figures 2U,V and S5F). In contrast to results observed in Phase 1, ORP remained stable (ca. −145 mV) (Figure 2E,F) during Phase 3. Across all wells, including control wells, groundwater sulfate concentrations increased and then decreased in Phase 3 (Figure S3). Groundwater sulfide concentrations did not substantially change during Phase 3. The stability of the ORP following the second oxygen injection (Phase 3) coincided with the introduction of oxidized species introduced during Phases 2–4, indicated by an increase in groundwater sulfate concentrations. Introduction of oxidized chemical species may have been due to upgradient flow or an aquifer recharge event.

Phase 4: Cessation of O_2 Delivery

The injection of oxygenated groundwater halted near day 75. Again, an increase in groundwater U concentrations was observed as well as a slight increase in groundwater Fe and Mn concentrations in accordance with the negative correlation with O_2 (Figures 3 and S2) similar to prior results (Figures 2M,N and S2). For a brief period from day 79–85, injection resumed, observable as a small peak in tracer concentrations in downgradient wells. In this short period, a small decrease in groundwater U was observed (Figures 2I,J and S5C). On day 85, injection was stopped for 5 days in order to refill the injection tank. It should be noted that we observed a decrease in

ORP (range −253.6– −213.5 mV) in all wells except CD11 on day 82 (Figures 2E–H and S5B). Dissolved inorganic carbon concentrations continued to fluctuate during Phase 4 (Figures 2U–W and S5F).

Phase 5: Response Following an Increase in O_2 Delivery Rate

The rate of oxgenated groundwater delivery into the aquifer was increased by 2.5 times from 21.6 mg O_2/h per injection well to 54 mg/h when the injection resumed on day 95 in order to determine whether the total amount of O_2 impacted U mobility. Despite the increase, groundwater DO remained suboxic (<0.2 mg/L), indicating near complete consumption of the introduced DO (Figure 2A,B). The ORP in all wells was observed to increase, ranging from −86.8 to +164.7 mV on day 101 (Figures 2E–H and S5B). This observation included unamended control wells CU01 and CD11 (Figures 2E–H and S5B). The rise in ORP was accompanied by a decrease in total Fe and groundwater pH in all wells and initially an increase in groundwater sulfate concentrations. The loss of total iron and increase in ORP and sulfate suggests the intrusion of oxidized species, possibly DO, from the capillary fringe following an aquifer recharge event or flow from upgradient. The increase was greatest in the upgradient well CU01, rising to +164.7 mV from −213.5 mV (Figure 2H). Groundwater U concentrations did not change in the upgradient well (Figure 2L). In the unamended acetate-reduced control well, CD11 groundwater U concentrations slightly increased by 15 µg/L (Figure 2K). In contrast to control wells CU01 and CD11, groundwater U concentrations substantially increased in all amended wells (Figures 2I–L and S5C), up to 124 µg/L. During Phase 5, as DO was consumed more groundwater U was released into solution (Figure 5). These results are opposite of the decrease in groundwater U when the rate of DO injection was low (Figure 5). Groundwater total Fe and Mn decreased with O_2 delivery (Figure S2). While groundwater sulfate concentrations were initially observed to increase, groundwater sulfate concentrations decreased to levels similar to those measured at the beginning of Phase 5. During this period, DOC concentrations diverged. In CD01, DOC increased to 10.4 mg/L, while in both CD18 and CD02, DOC decreased to 0 mg/L (Figures 2U–W and S5F). Groundwater DOC concentrations fluctuated in the upgradient well CU01, an increase to 6.2 mg/L then decreased to 3.6 mg/L (Figure 2W). There were slight increases in DIC in CD18 and CD01, but not in CD02, nor upgradient well CU01 (Figures 2U–W and S5F).

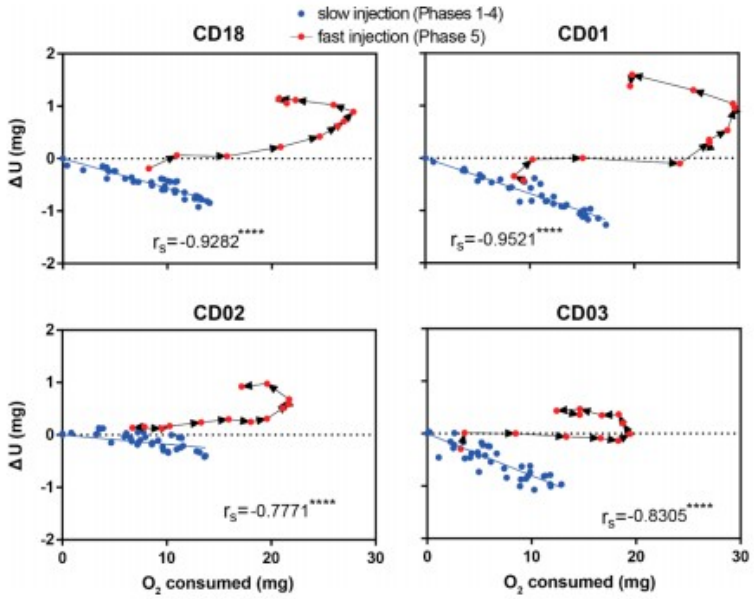

Figure 5. Groundwater U decreases with O_2 consumption during the slow injection phase (P1−4). When delivery of O_2 is increased during the fast injection phase, groundwater U increases. r_s denotes Spearman's correlation coefficient during the slow injection phase. Stars represent the degree of significance with a single star (*) representing $p < 0.05$, two stars (**) representing $p < 0.01$, three stars (***) representing $p < 0.001$, and four stars (****) representing $p < 0.0001$.

Discussion

Here our results indicate that the influx of oxygenated groundwater into a reduced system may not necessarily result in the mobilization of a redox sensitive contaminant such as uranium. Rather, subsurface bioreduced zones may serve as a geochemical trap and redox buffer upon the influx of low oxidant concentrations but can be overcome once a tipping point is reached. Here, biogeochemical dynamics following the initial injection of oxygenated groundwater into the previously bioreduced zone resulted in loss of aqueous U from groundwater. Reduced U minerals including biogenic uraninite are expected to be solubilized by oxidative dissolution coupled to the abiotic reduction of O_2.(21,23,26,62,63) Thus, an increase in aqueous U concentrations would have been expected due to chemical(23) or biological oxidation upon the influx of DO into the aquifer.(64,65) Rather, aqueous U concentrations were observed to decrease. Once the injection rate increased from 36 mL/h per injection well to 90 mL/h, representing an increase from 21.6 mg of O_2 delivered per hour to 54 mg/h, aqueous U concentrations increased, presumably as a result of oxidative dissolution of reduced U minerals. These results are consistent with prior results where oxidative U(IV) dissolution rates have been demonstrated to increase with increasing groundwater DO in the Rifle aquifer.(21) This indicates that high rates of DO infiltration above a threshold or “tipping point” can lead to U mobilization. This result may also explain the results reported in a meta-analysis where a single DO measurement was not significantly correlated with elevated groundwater U concentrations.(15) Instead, the delivery rate (or mass/unit time) of DO plays a significant role in controlling U mobility, such that the

contaminant retention either by (i) reduction or (ii) association with reactive Fe(III) oxide surfaces is overcome and U solubilization becomes favorable.

Reduced Regions As Redox Buffers Retaining Uranium

Throughout the experiment, DO delivered into the aquifer did not result in an increase in measurable groundwater DO, indicating immediate consumption within the bioreduced region of the aquifer. Reduced inorganic chemical species and minerals such as aqueous Fe(II) and FeS minerals respectively, complex organic matter, and detrital biomass may contribute to the oxidative buffering capacity providing sufficient reducing equivalents to remove an oxidant including DO from the system.(13,21) Thus, reduced regions can protect against the oxidation of reduced U(IV) minerals. The growth and activity of aerobic respiring microorganisms likely maintain anoxic conditions by the consumption of DO, and some fermenting species are also expected to increase upon exposure to oxygen.(66) These fermenters play a role in the decomposition of organic matter, generating labile forms more readily used by heterotrophs which may explain why DOC was observed to fluctuate after O_2 delivery. Biological consumption of DO, release of more labile forms of organic carbon, and decrease in U immediately after the initial period of O_2 delivery in Phase 1 could be explained by reductive processes. The liberation and increase of pools of labile organic carbon can thus serve as a microbial energy source which can be coupled to U respiration.(4) It is recognized that redox transitions between oxic and anoxic conditions enhance degradation of organic carbon as a result of microbial activity, releasing labile organic compounds.(67,68) Decomposition of recalcitrant organic matter in sediment is limited by the availability of electron acceptors particularly DO, which facilitates oxygen-dependent enzymatic cleaving of nonhydrolyzable bonds(20,67) or organic carbon oxidation coupled to the reduction of O_2.(68)

In addition, the delivery of O_2 may also reoxidize reduced Fe minerals formed during past biostimulation, which has been observed before in a series of column experiments with bioreduced sediment supplied with DO.(69) The production of reactive oxygen species, such as H_2O_2 and ·OH, has been observed at oxic–anoxic interfaces(70,71) including the Rifle aquifer. The production could be a result of aerobic respiration or oxidation of Fe(II). The oxidation of Fe(II) and subsequent formation of reactive Fe(III) oxide species may also produce reactive intermediates, such as superoxides, which could also catalyze the decomposition of organic matter,(72) further increasing organic carbon availability.

Reactive iron sulfide minerals as well as aqueous sulfide may also play a role in the observed oxidative buffering. Thus, reactive minerals and reduced ions in groundwater and aquifer sediment represent a potent abiotic scavenger of groundwater DO.(13,73−75) In some cases, they have been observed to prevent oxidation of U(IV),(76) but in other cases, iron sulfide scavenging of DO has been demonstrated to be too slow to prevent U(IV) oxidation(28) and

that Fe(II) oxidation occurs concurrently with U(IV) oxidation.(63) These conflicting reports may be explained by our findings which show a dependence on the rate of O_2 delivery. Abiotic reduction of U(VI) by Fe(II) may potentially account for some of the decrease in aqueous U during O_2 delivery.(77−79) The addition of Fe(III) oxide minerals has been previously demonstrated to increase U(VI) reduction rates via the biological reduction of Fe(III) generating a reductant for U(VI).(80)

Though the redox state of U plays a significant role controlling mobility, U(VI) incorporation into or sorption onto freshly precipitated metal oxides such as Fe(III) minerals could also account for a loss in groundwater U measured in this study during the injection of DO.(81−83) Uranium adsorption onto Fe(III) oxide minerals is a well-recognized process.(83) Though U will adsorb to Fe(III) oxide minerals at near neutral pH, carbonate ligands have been recognized to decrease U adsorption to Fe(III) oxides and thus drive U mobility.(77,84,85) Despite observed increases in DIC in wells CD01 and CU01 during Phase 1, groundwater U concentrations did not rise, rather they were observed to decrease (CD01) or remain unchanged (CU01). As such, these results are not consistent with adsorption as a primary mechanism controlling U mobility during the DO injection phase and the decrease in groundwater U concentrations. An alternative explanation is the incorporation of U into iron oxides. However, during Phase 5 when a significant loss of groundwater Fe was observed, (indicative of precipitation), U was released back into the groundwater. As such, U incorporation into Fe(III) oxides would not be the sole mechanism controlling U mobility in the aquifer.

Microbial and Viral Responses

Prior acetate injections increased microbial biomass in the aquifer and increased subsurface organic carbon. As such, microbial activity would be expected to be greater in the biostimulated region of the aquifer. Following intrusion of O_2 into a reduced zone, biomass growth and activity from aerobic heterotrophs, fermenters, nitrate reducers, sulfate reducers, and chemolithoautotrophs are expected.(66) Time-series metagenomic data collected from Rifle, CO during DO injection has shown that key metabolic processes including both anaerobic and aerobic respiration and C/N fixation were always present in microbial communities.(86) However, the abundance of metabolic genes varied with geochemical conditions.(86) The potential for aerobic respiration was present in 34% of the genomes from the subsurface, (86) so microbial communities likely shifted in response to the oxygen injection. Genes involved in iron cycling were also present, but only a few genomes possessed them, primarily deltaproteobacteria.(86)

Whereas planktonic cell abundances did not significantly change, significant increases in viral abundances were observed during Phase 1 after DO delivery. This interesting observation has implications for subsurface biogeochemical cycling. Viruses depend on active host cells for reproduction.

(87−90) As such, upon the influx of DO, an increase in microbial activity and growth is expected. Yet an increase in cell abundance was not observed, but may be a result of cell mediated lysis and viral production yielding an increase in VMR. Faster host growth has been associated with higher VMR.(91) Thus, shifts in VMR may be indicative of relative changes in host microbial activity resulting in virus production and cell lysis. The initial increases in VMR reported here indicate a bloom of viruses near the injection site resulting from active viral production and/or cell lysis. The observed increase in viruses is not likely to be a result of dislodgement of viruses from sediment due to increased groundwater velocity. At the rate of injection in the experiment, groundwater velocity would minimally increase relative to groundwater flow rates, no more than 240 mL/day faster in Phase 1. Because viral lysis could result in the liberation of labile organic carbon from cells and enhanced biomass turnover, the potential role of viruses has significant implications for subsurface metal/radionuclide cycling in subsurface sediments.(92) Viral lysis of actively growing cell populations may play a role in the cycling of metals and radionuclides by increasing pools of labile organic carbon which can subsequently be utilized by metal/radionuclide reducers and thus drive U immobilization.(38)

The observed decrease in groundwater viruses following the visible precipitation of minerals during Phase 2 can be explained by the formation of ferric oxyhydroxide precipitates.(93−95) The loss of free viruses can occur through physicochemical processes, such as adsorption to iron oxides or entrainment during mineral precipitation.(60,61,93,95,96) Conversely, some increase in free viruses may also come from desorption of attached viruses as a result of a change in groundwater geochemistry. As such, groundwater geochemical parameters that control formation of mineral sorbents are expected to strongly impact virus–host interactions that influence microbial activity and microbial community structure. Because only groundwater was collected here, the abundances of sediment-associated viruses were not possible to determine. However, the initial increases in groundwater virus abundance observed here are in accordance with previous observations of virus blooms following stimulation of microbial activity in aquifer sediments by supplying of an electron donor and acceptor.(29) Further research is needed to describe mechanisms that influence viral abundances following geochemical perturbations to subsurface systems as well as their consequences for subsurface biogeochemical cycling.

Environmental Significance

These results have implications for the stability of reduced U present in bioreduced regions. The results shown here indicate that oxidant influx exceeding a certain influx rate or threshold concentration can overcome the redox buffering–sequestration capacity of sediments potentially leading to mobilization of U. Thus, it would also be expected that natural influxes of elevated O_2concentrations can also play a role oxidizing minerals sequestered in these bioreduced zones. Seasonal fluctuations of the water

table can lead to signficant variation of DO (0.1 to 4–5 mg/L) due to O_2 transport from the capillary fringe.(11) Using well CD01 as an example, results indicte that if the influx rate did not pass the threshold, it may potentially lead to sequestration of up to 256–320 μg/L of U due to seasonal fluctuation of the water table. However, past the threshold, the release of U may be expected. Climate-induced hydrological changes and events could also lead to significant changes in the water table level(97) exposing reduced sediments to greater concentrations of oxidants(98) and mobilizing U.(21,26,63) Anthropogenic groundwater withdrawls could also alter subsurface flow rates,(99) increasing the mass of oxidants(98) introduced into reduced sediments where heavy metals such as U are geochemically trapped. Thus, anthropogenic withdrawl could also catalyze mobilization of U in naturally reduced sediments.

Buried naturally reduced sediment lenses are present at the Rifle aquifer and common in aquifers across the Upper Colorado River Basin and predicted to be important contributors to regional biogeochemical processes despite comprising only a fraction of the volume of alluvial aquifers.(4−6,100) The bioreduced sediments are in various ways similar to buried naturally reduced sediments. They are both highly reduced zones with abundant iron sulfide minerals and where U(IV) minerals are concentrated.(4,42) Because of the similarity between bioreduced sediments and naturally reduced sediments, naturally reduced sediments thus may also behave in a similar manner. (4) Intrusion of dissolved oxygen into naturally reduced sediments by a rising water table have been observed to result in reoxidation and/or mobilization of U.(13) Additional studies are required in order to examine the fate of reduced metals and organic carbon in zones that have not been augmented with labile organic carbon. Additionally, assumptions of constant rates of biomass turnover used to model carbon and metal/radionuclide biogeochemistry may have to be reconsidered linking viral mediated cell lysis.(13,46) We suggest that future experiments and modeling of contaminant transport at redox interfaces consider the concentration of oxidants transported to the redox interface and the incorporation of biotic processes influenced by viral predation and transformations of organic matter.

Acknowledgments

U.S. Department of Energy (DOE), Office of Science, Office of Biological and Environmental Research funded the work under contracts DE-SC0004113 (K.A.W., University of Nebraska–Lincoln) and DE-AC02-05CH11231 (Lawrence Berkeley National Laboratory; operated by the University of California). This material is partially based upon work supported through the Lawrence Berkeley National Laboratory’s Sustainable Systems Scientific Focus Area. Additional support for provided by the United States Geological Survey 104g Program (2014NE265G) and National Science Foundation IGERT Fellowship (0903469) for K.A.W. and D.P., respectively.

References

This article references 100 other publications.

(1) Blazejewski, G. A.; Stolt, M. H.; Gold, A. J.; Gurwick, N.; Groffman, P. M. Spatial distribution of carbon in the subsurface of riparian zones. Soil Sci. Soc. Am. J. 2009, 73 (5), 1733−1740. (2) Blazejewski, G. A.; Stolt, M. H.; Gold, A. J.; Groffman, P. M. Macro-and micromorphology of subsurface carbon in riparian zone soils. Soil Sci. Soc. Am. J. 2005, 69 (4), 1320−1329. (3) McClain, M. E.; Boyer, E. W.; Dent, C. L.; Gergel, S. E.; Grimm, N. B.; Groffman, P. M.; Hart, S. C.; Harvey, J. W.; Johnston, C. A.; Mayorga, E.; McDowell, W. H.; Pinay, G. Biogeochemical hot spots and hot moments at the interface of terrestrial and aquatic ecosystems. Ecosystems 2003, 6 (4), 301−312. (4) Campbell, K. M.; Kukkadapu, R. K.; Qafoku, N.; Peacock, A. D.; Lesher, E.; Williams, K. H.; Bargar, J. R.; Wilkins, M. J.; Figueroa, L.; Ranville, J.; Davis, J. A.; Long, P. E. Geochemical, mineralogical and microbiological characteristics of sediment from a naturally reduced zone in a uranium-contaminated aquifer. Appl. Geochem. 2012, 27 (8), 1499−1511. (5) Qafoku, N. P.; Kukkadapu, R. K.; McKinley, J. P.; Arey, B. W.; Kelly, S. D.; Wang, C.; Resch, C. T.; Long, P. E. Uranium in framboidal pyrite from a naturally bioreduced alluvial sediment. Environ. Sci. Technol. 2009, 43 (22), 8528−8534. (6) Qafoku, N. P.; Gartman, B. N.; Kukkadapu, R. K.; Arey, B. W.; Williams, K. H.; Mouser, P. J.; Heald, S. M.; Bargar, J. R.; Janot, N.; Yabusaki, S.; Long, P. E. Geochemical and mineralogical investigation of uranium in multi-element contaminated, organic-rich subsurface sediment. Appl. Geochem. 2014, 42, 77−85. (7) McDonald, C. Discussion: status, directions and R&D issues. In Advanced groundwater remediation: Active and passive technologies; Simon, F. G., Meggyes, T., McDonald, C., Eds.; Thomas Telford Publishing: London, 2002; Chapter 19, pp 303−325. (8) Williams, K. H.; Long, P. E.; Davis, J. A.; Wilkins, M. J.; N’Guessan, A. L.; Steefel, C. I.; Yang, L.; Newcomer, D.; Spane, F. A.; Kerkhof, L. J.; McGuinness, L.; Dayvault, R.; Lovley, D. R. Acetate Availability and its Influence on Sustainable Bioremediation of Uranium-Contaminated Groundwater. Geomicrobiol. J. 2011, 28 (5− 6), 519−539. (9) Anderson, R. T.; Vrionis, H. A.; Ortiz-Bernad, I.; Resch, C. T.; Long, P. E.; Dayvault, R.; Karp, K.; Marutzky, S.; Metzler, D. R.; Peacock, A.; White, D. C.; Lowe, M.; Lovley, D. R. Stimulating the in situ activity of Geobacter species to remove uranium from the groundwater of a uranium-contaminated aquifer. Appl. Environ. Microbiol. 2003, 69 (10), 5884−91. (10) Yelton, A. P.; Williams, K. H.; Fournelle, J.; Wrighton, K. C.; Handley, K. M.; Banfield, J. F. Vanadate and acetate biostimulation of contaminated sediments decreases diversity, selects for specific taxa, and decreases aqueous V5+ concentration. Environ. Sci. Technol. 2013, 47 (12), 6500−9. (11) Zachara, J. M.; Long, P. E.; Bargar, J.; Davis, J. A.; Fox, P.; Fredrickson, J. K.; Freshley, M. D.; Konopka, A. E.; Liu, C.; McKinley, J. P.; Rockhold, M. L.; Williams, K. H.; Yabusaki, S. B. Persistence of uranium groundwater plumes: Contrasting mechanisms at two DOE sites in the groundwater−river interaction zone. J. Contam. Hydrol. 2013, 147, 45−72.

(12) Newsome, L.; Morris, K.; Shaw, S.; Trivedi, D.; Lloyd, J. R. The stability of microbially reduced U(IV); impact of residual electron donor and sediment ageing. Chem. Geol. 2015, 409, 125−135. (13) Danczak, R. E.; Yabusaki, S. B.; Williams, K. H.; Fang, Y.; Hobson, C.; Wilkins, M. J. Snowmelt induced hydrologic perturbations drive dynamic microbiological and geochemical behaviors across a shallow riparian aquifer. Front. Earth Sci. 2016, 4, 57. (14) Nolan, B. T.; Hitt, K. J.; Ruddy, B. C. Probability of nitrate contamination of recently recharged groundwaters in the conterminous United States. Environ. Sci. Technol. 2002, 36 (10), 2138−2145. (15) Nolan, J.; Weber, K. A. Natural Uranium Contamination in Major U.S. Aquifers Linked to Nitrate. Environ. Sci. Technol. Lett. 2015, 2 (8), 215−220. (16) Haberer, C. M.; Rolle, M.; Liu, S.; Cirpka, O. A.; Grathwohl, P. A high-resolution non-invasive approach to quantify oxygen transport across the capillary fringe and within the underlying groundwater. J. Contam. Hydrol. 2011, 122 (1), 26−39. (17) Ha, J.-H.; Seagren, E. A.; Song, X. Oxygen Transport across the Capillary Fringe in LNAPL Pool-Source Zones. J. Environ. Eng. 2014, 140 (12), 04014040. (18) Lee, C. Controls on organic carbon preservation: The use of stratified water bodies to compare intrinsic rates of decomposition in oxic and anoxic systems. Geochim. Cosmochim. Acta 1992, 56 (8), 3323−3335. (19) Keil, R. G.; Hu, F. S.; Tsamakis, E. C.; Hedges, J. I. Pollen in marine sediments as an indicator of oxidation of organic matter. Nature 1994, 369 (6482), 639−641. (20) Burdige, D. J. Preservation of organic matter in marine sediments: controls, mechanisms, and an imbalance in sediment organic carbon budgets? Chem. Rev. 2007, 107 (2), 467−485. (21) Campbell, K. M.; Veeramani, H.; Ulrich, K.-U.; Blue, L. Y.; Giammar, D. E.; Bernier-Latmani, R.; Stubbs, J. E.; Suvorova, E.; Yabusaki, S.; Lezama-Pacheco, J. S.; Mehta, A.; Long, P. E.; Bargar, J. R. Oxidative dissolution of biogenic uraninite in groundwater at Old Rifle, CO. Environ. Sci. Technol. 2011, 45 (20), 8748−8754. (22) Amano, Y.; Sasao, E.; Niizato, T.; Iwatsuki, T. Redox Buffer Capacity in Water-Rock-Microbe Interaction Systems in Subsurface Environments. Geomicrobiol. J. 2012, 29 (7), 628−639. (23) Langmuir, D. Uranium solution-mineral equilibria at low temperatures with applications to sedimentary ore deposits. Geochim. Cosmochim. Acta 1978, 42 (6), 547−569. (24) Senko, J. M.; Istok, J. D.; Suflita, J. M.; Krumholz, L. R. In-situ evidence for uranium immobilization and remobilization. Environ. Sci. Technol. 2002, 36 (7), 1491−1496. (25) Moon, H.; Komlos, J.; Jaffe, P. Biogenic U (IV) oxidation by dissolved oxygen and nitrate in sediment after prolonged U (VI)/Fe (III)/SO4 2− reduction. J. Contam. Hydrol. 2009, 105 (1), 18−27. (26) Wu, W.-M.; Carley, J.; Luo, J.; Ginder-Vogel, M. A.; Cardenas, E.; Leigh, M. B.; Hwang, C.; Kelly, S. D.; Ruan, C.; Wu, L. In situ bioreduction of uranium (VI) to submicromolar levels and reoxidation by dissolved oxygen. Environ. Sci. Technol. 2007, 41 (16), 5716−5723. (27) Komlos, J.; Peacock, A.; Kukkadapu, R. K.; Jaffe, P. R. Long-´ term dynamics of uranium reduction/reoxidation under low sulfate conditions. Geochim. Cosmochim. Acta 2008, 72 (15), 3603−3615. (28) N’Guessan, A. L.; Moon, H. S.; Peacock, A. D.; Tan, H.; Sinha, M.; Long, P. E.; Jaffe, P. R. Postbiostimulation microbial

community′ structure changes that control the reoxidation of uranium. FEMS Microbiol. Ecol. 2010, 74 (1), 184−195. (29) Pan, D.; Watson, R.; Wang, D.; Tan, Z. H.; Snow, D. D.; Weber, K. A. Correlation between viral production and carbon mineralization under nitrate-reducing conditions in aquifer sediment. ISME J. 2014, 8 (8), 1691. (30) Middelboe, M.; Lyck, P. G. Regeneration of dissolved organic matter by viral lysis in marine microbial communities. Aquat. Microb. Ecol. 2002, 27 (2), 187−194. (31) Weitz, J. S.; Wilhelm, S. W. Ocean viruses and their effects on microbial communities and biogeochemical cycles. F1000 Biol. Rep. 2012, 4, 17. (32) Fuhrman, J. A. Marine viruses and their biogeochemical and ecological effects. Nature 1999, 399, 541. (33) Ghosh, D.; Roy, K.; Williamson, K. E.; Srinivasiah, S.; Wommack, K. E.; Radosevich, M. Acyl-homoserine lactones can induce virus production in lysogenic bacteria: an alternative paradigm for prophage induction. Appl. Environ. Microbiol. 2009, 75 (22), 7142−7152. (34) Srinivasiah, S. In situ and in vitro evaluation of viral-host dynamics in soils and uranium-contaminated subsurface aquifers. University of Delaware, 2011. (35) Pan, D.; Nolan, J.; Williams, K. H.; Robbins, M. J.; Weber, K. A. Abundance and Distribution of Microbial Cells and Viruses in an Alluvial Aquifer. Front. Microbiol. 2017, 8, 1199. (36) Wrighton, K. C.; Thomas, B. C.; Sharon, I.; Miller, C. S.; Castelle, C. J.; VerBerkmoes, N. C.; Wilkins, M. J.; Hettich, R. L.; Lipton, M. S.; Williams, K. H.; Long, P. E.; Banfield, J. F. Fermentation, hydrogen, and sulfur metabolism in multiple uncultivated bacterial phyla. Science 2012, 337 (6102), 1661−5. (37) Wrighton, K. C.; Castelle, C. J.; Wilkins, M. J.; Hug, L. A.; Sharon, I.; Thomas, B. C.; Handley, K. M.; Mullin, S. W.; Nicora, C. D.; Singh, A.; Lipton, M. S.; Long, P. E.; Williams, K. H.; Banfield, J. F. Metabolic interdependencies between phylogenetically novel fermenters and respiratory organisms in an unconfined aquifer. ISME J. 2014, 8, 1452. (38) Holmes, D. E.; Giloteaux, L.; Chaurasia, A. K.; Williams, K. H.; Luef, B.; Wilkins, M. J.; Wrighton, K. C.; Thompson, C. A.; Comolli, L. R.; Lovley, D. R. Evidence of Geobacter-associated phage in a uranium-contaminated aquifer. ISME J. 2015, 9 (2), 333−346. (39) Comolli, L. R.; Duarte, R.; Baum, D.; Luef, B.; Downing, K. H.; Larson, D. M.; Csencsits, R.; Banfield, J. F. A portable cryo-plunger for on-site intact cryogenic microscopy sample preparation in natural environments. Microsc. Res. Tech. 2012, 75 (6), 829−836. (40) Kyle, J. E.; Eydal, H. S.; Ferris, F. G.; Pedersen, K. Viruses in granitic groundwater from 69 to 450 m depth of the Ä spöhard rock laboratory, Sweden. ISME J. 2008, 2 (5), 571−574. (41) Roudnew, B.; Seymour, J. R.; Jeffries, T. C.; Lavery, T. J.; Smith, R. J.; Mitchell, J. G. Bacterial and Virus-Like Particle Abundances in Purged and Unpurged Groundwater Depth Profiles. Groundwater Monit. Rem. 2012, 32 (4), 72−77. (42) Janot, N.; Lezama Pacheco, J. S.; Pham, D. Q.; O'Brien, T. M.; Hausladen, D.; Noel, V.; Lallier, F.; Maher, K.; Fendorf, S.; Williams,¨ K. H.; Long, P. E.; Bargar, J. R. Physico-chemical heterogeneity of organic-rich sediments in the Rifle aquifer, CO: Impact on uranium biogeochemistry. Environ. Sci. Technol. 2016, 50 (1), 46−53. (43) Li, L.; Steefel, C. I.; Williams, K. H.; Wilkins, M. J.; Hubbard, S. S. Mineral transformation and biomass accumulation associated with uranium

bioremediation at Rifle, Colorado. Environ. Sci. Technol. 2009, 43 (14), 5429−5435. (44) Li, L.; Steefel, C. I.; Kowalsky, M. B.; Englert, A.; Hubbard, S. S. Effects of physical and geochemical heterogeneities on mineral transformation and biomass accumulation during biostimulation experiments at Rifle, Colorado. J. Contam. Hydrol. 2010, 112 (1), 45−63. (45) Vrionis, H. A.; Anderson, R. T.; Ortiz-Bernad, I.; O'Neill, K. R.; Resch, C. T.; Peacock, A. D.; Dayvault, R.; White, D. C.; Long, P. E.; Lovley, D. R. Microbiological and geochemical heterogeneity in an in situ uranium bioremediation field site. Appl. Environ. Microbiol. 2005, 71 (10), 6308−18. (46) Yabusaki, S. B.; Fang, Y.; Williams, K. H.; Murray, C. J.; Ward, A. L.; Dayvault, R. D.; Waichler, S. R.; Newcomer, D. R.; Spane, F. A.; Long, P. E. Variably saturated flow and multicomponent biogeochemical reactive transport modeling of a uranium bioremediation field experiment. J. Contam. Hydrol. 2011, 126 (3), 271−290. (47) Englert, A.; Hubbard, S.; Williams, K.; Li, L.; Steefel, C. Feedbacks between hydrological heterogeneity and bioremediation induced biogeochemical transformations. Environ. Sci. Technol. 2009, 43 (14), 5197−5204. (48) Luef, B.; Frischkorn, K. R.; Wrighton, K. C.; Holman, H.-Y. N.; Birarda, G.; Thomas, B. C.; Singh, A.; Williams, K. H.; Siegerist, C. E.; Tringe, S. G.; Downing, K. H.; Comolli, L. R.; Banfield, J. F. Diverse uncultivated ultra-small bacterial cells in groundwater. Nat. Commun. 2015, 6, 6372. (49) Long, P. E.; Williams, K. H.; Davis, J. A.; Fox, P. M.; Wilkins, M. J.; Yabusaki, S. B.; Fang, Y.; Waichler, S. R.; Berman, E. S.; Gupta, M.; Chandler, D. P.; Murray, C.; Peacock, A. D.; Giloteaux, L.; Handley, K. M.; Lovley, D. R.; Banfield, J. F. Bicarbonate impact on U(VI) bioreduction in a shallow alluvial aquifer. Geochim. Cosmochim. Acta 2015, 150, 106−124. (50) Bao, C.; Wu, H.; Li, L.; Newcomer, D.; Long, P. E.; Williams, K. H. Uranium bioreduction rates across scales: biogeochemical hot moments and hot spots during a biostimulation experiment at Rifle, Colorado. Environ. Sci. Technol. 2014, 48 (17), 10116−10127. (51) Potter, B.; Wimsatt, J. Method 415.3: Determination of total organic carbon and specific UV absorbance at 254 nm in source water and drinking water; U.S. Environmental Protection Agency: Cincinnati, OH, 2005. (52) Hautman, D. P.; Munch, D. J. Method 300.1: Determination of inorganic anions in drinking water by ion chromatography; U.S. Environmental Protection Agency: Cincinnati, OH, 1997. (53) Kantor, R. S.; Wrighton, K. C.; Handley, K. M.; Sharon, I.; Hug, L. A.; Castelle, C. J.; Thomas, B. C.; Banfield, J. F. Small genomes and sparse metabolisms of sediment-associated bacteria from four candidate phyla. mBio 2013, 4 (5), e00708. (54) Harvey, A. E., Jr; Smart, J. A.; Amis, E. Simultaneous spectrophotometric determination of iron (II) and total iron with 1, 10-phenanthroline. Anal. Chem. 1955, 27 (1), 26−29. (55) Fogo, J. K.; Popowsky, M. Spectrophotometric determination of hydrogen sulfide. Anal. Chem. 1949, 21 (6), 732−734. (56) Brussaard, C. D. Enumeration of Bacteriophages Using Flow Cytometry. In Bacteriophages; Clokie, M. J., Kropinski, A., Eds.; Humana Press: New York, 2009; Vol. 501, pp 97−111. (57) Patel, A.; Noble, R. T.; Steele, J. A.; Schwalbach, M. S.; Hewson, I.; Fuhrman, J. A. Virus and prokaryote enumeration from planktonic aquatic environments by

epifluorescence microscopy with SYBR Green I. Nat. Protoc. 2007, 2 (2), 269−276. (58) Parikka, K. J.; Le Romancer, M.; Wauters, N.; Jacquet, S. Deciphering the virus-to-prokaryote ratio (VPR): insights into virus− host relationships in a variety of ecosystems. Biol. Rev. 2017, 92 (2), 1081−1100. (59) Cornell, R. M.; Schwertmann, U. The iron oxides: structure, properties, reactions, occurrences and uses; John Wiley & Sons: Hoboken, NJ, 2006. (60) You, Y.; Han, J.; Chiu, P. C.; Jin, Y. Removal and inactivation of waterborne viruses using zerovalent iron. Environ. Sci. Technol. 2005, 39 (23), 9263−9. (61) Nieto-Juarez, J. I.; Kohn, T. Virus removal and inactivation by iron (hydr)oxide-mediated Fenton-like processes under sunlight and in the dark. Photochemical & photobiological sciences: Official journal of the European Photochemistry Association and the European Society for Photobiology 2013, 12 (9), 1596−605. (62) Maher, K.; Bargar, J. R.; Brown, G. E., Jr Environmental speciation of actinides. Inorg. Chem. 2013, 52 (7), 3510−3532. (63) Moon, H. S.; Komlos, J.; Jaffe, P. R. Uranium reoxidation in´ previously bioreduced sediment by dissolved oxygen and nitrate. Environ. Sci. Technol. 2007, 41 (13), 4587−4592. (64) Emerson, D. Microbial oxidation of Fe (II) and Mn (II) at circumneutral pH. Environmental Microbe-Metal Interactions 2000, 31−52. (65) Emerson, D.; Weiss, J. V. Bacterial iron oxidation in circumneutral freshwater habitats: findings from the field and the laboratory. Geomicrobiol. J. 2004, 21 (6), 405−414. (66) Yabusaki, S. B.; Wilkins, M. J.; Fang, Y.; Williams, K. H.; Arora, B.; Bargar, J.; Beller, H. R.; Bouskill, N. J.; Brodie, E. L.; Christensen, J. N.; Conrad, M. E.; Danczak, R. E.; King, E.; Soltanian, M. R.; Spycher, N. F.; Steefel, C. I.; Tokunaga, T. K.; Versteeg, R.; Waichler, S. R.; Wainwright, H. M. Water Table Dynamics and Biogeochemical Cycling in a Shallow, Variably-Saturated Floodplain. Environ. Sci. Technol. 2017, 51 (6), 3307−3317. (67) Kristensen, E.; Ahmed, S. I.; Devol, A. H. Aerobic and anaerobic decomposition of organic matter in marine sediment: which is fastest? Limnol. Oceanogr. 1995, 40 (8), 1430−1437. (68) Hulthe, G.; Hulth, S.; Hall, P. O. Effect of oxygen on degradation rate of refractory and labile organic matter in continental margin sediments. Geochim. Cosmochim. Acta 1998, 62 (8), 1319− 1328. (69) Komlos, J.; Kukkadapu, R. K.; Zachara, J. M.; Jaffe, P. R.´ Biostimulation of iron reduction and subsequent oxidation of sediment containing Fe-silicates and Fe-oxides: Effect of redox cycling on Fe(III) bioreduction. Water Res. 2007, 41 (13), 2996− 3004. (70) Yuan, X.; Nico, P. S.; Huang, X.; Liu, T.; Ulrich, C.; Williams, K. H.; Davis, J. A. Production of Hydrogen Peroxide in Groundwater at Rifle, Colorado. Environ. Sci. Technol. 2017, 51 (14), 7881−7891. (71) Page, S. E.; Kling, G. W.; Sander, M.; Harrold, K. H.; Logan, J. R.; McNeill, K.; Cory, R. M. Dark Formation of Hydroxyl Radical in Arctic Soil and Surface Waters. Environ. Sci. Technol. 2013, 47 (22), 12860−12867. (72) Hall, S. J.; Silver, W. L. Iron oxidation stimulates organic matter decomposition in humid tropical forest soils. Glob. Change Biol. 2013, 19 (9), 2804−2813. (73) Hyun, S. P.; Davis, J. A.; Sun, K.; Hayes, K. F. Uranium (VI) reduction by iron (II) monosulfide mackinawite. Environ. Sci. Technol. 2012, 46 (6), 3369−3376. (74) Gallegos, T. J.; Fuller, C. C.; Webb, S. M.; Betterton,

W. Uranium (VI) Interactions with Mackinawite in the Presence and Absence of Bicarbonate and Oxygen. Environ. Sci. Technol. 2013, 47 (13), 7357−7364. (75) Hyun, S. P.; Davis, J. A.; Hayes, K. F. Abiotic U(VI) reduction by aqueous sulfide. Appl. Geochem. 2014, 50, 7−15. (76) Carpenter, J.; Bi, Y.; Hayes, K. F. Influence of Iron Sulfides on Abiotic Oxidation of UO2 by Nitrite and Dissolved Oxygen in Natural Sediments. Environ. Sci. Technol. 2015, 49 (2), 1078−1085. (77) Waite, T.; Davis, J.; Payne, T.; Waychunas, G.; Xu, N. Uranium (VI) adsorption to ferrihydrite: Application of a surface complexation model. Geochim. Cosmochim. Acta 1994, 58 (24), 5465−5478. (78) Latta, D. E.; Boyanov, M. I.; Kemner, K. M.; O'Loughlin, E. J.; Scherer, M. M. Abiotic reduction of uranium by Fe (II) in soil. Appl. Geochem. 2012, 27 (8), 1512−1524. (79) Ginder-Vogel, M.; Criddle, C. S.; Fendorf, S. Thermodynamic Constraints on the Oxidation of Biogenic UO2 by Fe(III) (Hydr)- oxides. Environ. Sci. Technol. 2006, 40 (11), 3544−3550. (80) Jeon, B.-H.; Dempsey, B. A.; Burgos, W. D.; Barnett, M. O.; Roden, E. E. Chemical Reduction of U(VI) by Fe(II) at the Solid− Water Interface Using Natural and Synthetic Fe(III) Oxides. Environ. Sci. Technol. 2005, 39 (15), 5642−5649. (81) Lack, J. G.; Chaudhuri, S. K.; Kelly, S. D.; Kemner, K. M.; O'Connor, S. M.; Coates, J. D. Immobilization of Radionuclides and Heavy Metals through Anaerobic Bio-Oxidation of Fe(II). Appl. Environ. Microbiol. 2002, 68 (6), 2704−2710. (82) Nico, P. S.; Stewart, B. D.; Fendorf, S. Incorporation of Oxidized Uranium into Fe (Hydr)oxides during Fe(II) Catalyzed Remineralization. Environ. Sci. Technol. 2009, 43 (19), 7391−7396. (83) Cumberland, S. A.; Douglas, G.; Grice, K.; Moreau, J. W. Uranium mobility in organic matter-rich sediments: A review of geological and geochemical processes. Earth-Sci. Rev. 2016, 159, 160− 185. (84) Wazne, M.; Korfiatis, G. P.; Meng, X. Carbonate Effects on Hexavalent Uranium Adsorption by Iron Oxyhydroxide. Environ. Sci. Technol. 2003, 37 (16), 3619−3624. (85) Davis, J. A.; Meece, D. E.; Kohler, M.; Curtis, G. P. Approaches to surface complexation modeling of Uranium(VI) adsorption on aquifer sediments. Geochim. Cosmochim. Acta 2004, 68 (18), 3621− 3641. (86) Anantharaman, K.; Brown, C. T.; Hug, L. A.; Sharon, I.; Castelle, C. J.; Probst, A. J.; Thomas, B. C.; Singh, A.; Wilkins, M. J.; Karaoz, U.; Brodie, E. L.; Williams, K. H.; Hubbard, S. S.; Banfield, J. F. Thousands of microbial genomes shed light on interconnected biogeochemical processes in an aquifer system. Nat. Commun. 2016, 7, 13219. (87) Ashelford, K. E.; Norris, S. J.; Fry, J. C.; Bailey, M. J.; Day, M. J. Seasonal Population Dynamics and Interactions of Competing Bacteriophages and Their Host in the Rhizosphere. Appl. Environ. Microbiol. 2000, 66 (10), 4193−4199. (88) Germida, J. J. Population dynamics of Azospirillum brasilense and its bacteriophage in soil. Plant Soil 1986, 90 (1−3), 117−128. (89) Marsh, P.; Wellington, E. M. H. Phage-host interactions in soil. FEMS Microbiol. Ecol. 1994, 15 (1−2), 99−107. (90) Pantastico-Caldas, M.; Duncan, K. E.; Istock, C. A.; Bell, J. A. Population dynamics of bacteriophage and Bacillus subtilis in soil. Ecology 1992, 73, 1888−1902. (91) Wilcox, R. M.; Fuhrman, J. A. Bacterial viruses in coastal seawater: lytic rather than lysogenic production. Mar. Ecol.: Prog. Ser. 1994, 114, 35−35. (92) Suttle, C. A. Marine viruses–

major players in the global ecosystem. Nat. Rev. Microbiol. 2007, 5 (10), 801−12. (93) Schijven, J. F.; Medema, G.; Vogelaar, A. J.; Hassanizadeh, S. M. Removal of microorganisms by deep well injection. J. Contam. Hydrol. 2000, 44 (3), 301−327. (94) Loveland, J.; Ryan, J.; Amy, G.; Harvey, R. The reversibility of virus attachment to mineral surfaces. Colloids Surf., A 1996, 107, 205− 221. (95) Daughney, C. J.; Chatellier, X.; Chan, A.; Kenward, P.; Fortin,ˆ D.; Suttle, C. A.; Fowle, D. A. Adsorption and precipitation of iron from seawater on a marine bacteriophage (PWH3A-P1). Mar. Chem. 2004, 91 (1), 101−115. (96) Kyle, J. E.; Pedersen, K.; Ferris, F. G. Virus mineralization at low pH in the Rio Tinto, Spain. Geomicrobiol. J. 2008, 25 (7−8), 338−345. (97) Green, T. R.; Taniguchi, M.; Kooi, H.; Gurdak, J. J.; Allen, D. M.; Hiscock, K. M.; Treidel, H.; Aureli, A. Beneath the surface of global change: Impacts of climate change on groundwater. J. Hydrol. 2011, 405 (3), 532−560. (98) Zheng, Y.; Stute, M.; Van Geen, A.; Gavrieli, I.; Dhar, R.; Simpson, H.; Schlosser, P.; Ahmed, K. Redox control of arsenic mobilization in Bangladesh groundwater. Appl. Geochem. 2004, 19 (2), 201−214. (99) Alley, W. M.; Healy, R. W.; LaBaugh, J. W.; Reilly, T. E. Flow and storage in groundwater systems. Science 2002, 296 (5575), 1985− 1990. (100) Wainwright, H. M.; Flores Orozco, A.; Bücker, M.; Dafflon, B.; Chen, J.; Hubbard, S. S.; Williams, K. H. Hierarchical Bayesian method for mapping biogeochemical hot spots using induced polarization imaging. Water Resour. Res. 2016, 52 (1), 533−551.